

Initial Deflection Measurement of Continuous Plates in Actual Ships Using 3D Laser Scanner ^{*1}

Fumiya KAWASHIMA^{*}, Akira TATSUMI^{*}, Kazuhiro IJIMA^{*}
Daisuke SHIOMITSU^{**}, Fuminori YANAGIMOTO^{**}, Kinya ISHIBASHI^{**}

1. INTRODUCTION

When stiffeners are attached to plating by fillet welding, hungry-horse initial deflection is induced in the plate between the stiffeners due to thermal shrinkage. This initial deflection is an uncertain factor that significantly affects the buckling and ultimate strength of the stiffened panel structure. To investigate the characteristics of this initial deflection in welding, measurements of actual ships have been conducted for many years ¹⁻⁴). Contact-type displacement meters were used in those measurements, but because shape measurement is time-consuming, a sufficient volume of data has not been accumulated. Furthermore, the component of initial deflection that affects the buckling of the plate is the antisymmetric component with the stiffener. Therefore, the initial deflections of two adjacent rectangular plates are required in order to analyze this antisymmetric initial deflection, but the available data are minimal ⁴).

Recently, 3D laser scanners have been used to measure the shapes of structures ⁵), and one of the authors demonstrated the effectiveness of measuring the initial deflections of a box girder test specimen using a 3D laser scanner⁶). In this study, we apply a 3D laser scanner to measure the initial deflection of actual ships and investigate its applicability. The obtained initial deflection measurement data are analyzed to examine the correlation of the initial deflection components of two adjacent rectangular plates. Additionally, the statistical model of the initial deflection proposed in our previous studies ⁷⁻⁹) is extended to consider the correlation between adjacent plates.

2. MEASUREMENT OF INITIAL DEFLECTION

2.1 Measurement Targets

The initial deflection measurements were conducted at the Marugame Headquarters of Imabari Shipbuilding Co., Ltd. in 2023. The measured ships were a 64,000 DWT bulk carrier and a 5,800 TEU container ship. For the 64,000 DWT bulk carrier, the initial deflection of the side shell and bottom plating were measured, while for the 5,800 TEU container ship, the side shell and longitudinal bulkhead were measured.

2.2 Measurement Equipment

The 3D laser scanner Focus3D X130 manufactured by FARO Technologies Inc. was used in the measurements. This is a portable 3D laser scanner that measures surrounding objects as three-dimensional point cloud data. The measurement ranging error in the specification sheet is ± 2 mm.

^{*1} This paper is a reprint (with partial revisions) of a paper pp. 632-639 of the Conference Proceedings of the 37th Asian-Pacific Technical Exchange and Advisory Meeting on Marine Structures (TEAM2024), which was written by the authors and is published here with the approval of that organization.

^{*} Graduate School of Engineering, Osaka University

^{**} Research Institute, Research and Development Division, ClassNK

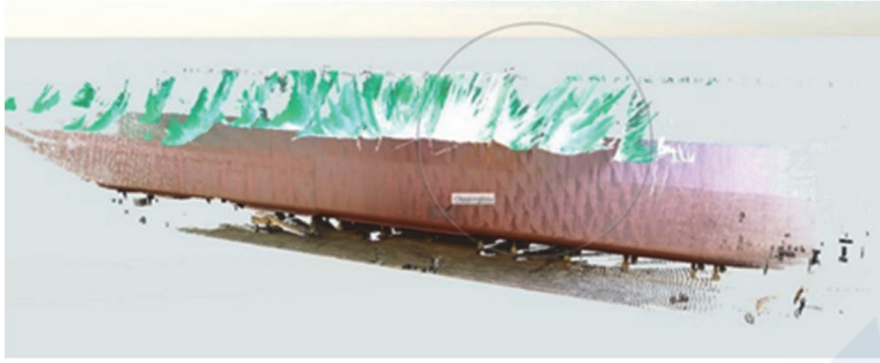


Fig. 1 Example of point cloud data of the ship side

2.3 Point Cloud Visualization

The point cloud data measured by the 3D laser scanner were visualized by using the software application FARO SCENE. Fig. 1 shows the visualized point cloud of the side of the 64,000 DWT bulk carrier. The target rectangular plates were extracted from this point cloud, the dispersion of the point cloud was checked, and the feasibility of analyzing the initial deflection was determined.

For the bottom of the bulk carrier, measurements of hull blocks on foundations were carried out with the laser scanner placed on the ground. However, due to the short distance between the scanner and the measurement target, the laser incidence angle increased at positions further from the scanner, which prevented accurate measurement of the initial deflection shape of the plates. For the side of the container ship, because measurements were carried out from the dockside, the distance between the measurement target and the scanner was long, resulting in significant dispersion in the point cloud.

In this study, the side shell of the bilge hopper tanks of the bulk carrier and the longitudinal bulkheads of the container ship, which could be measured accurately, were used for the initial deflection analysis. For the side of the bulk carrier, 21 pairs of adjacent rectangular plates, totaling 42 rectangular plates, were analyzed. For the longitudinal bulkheads of the container ship, 4 sets of 3 adjacent rectangular plates and 4 pairs of 2 adjacent rectangular plates, totaling 20 rectangular plates, were analyzed.

3. ANALYSIS OF INITIAL DEFLECTION

3.1 Analysis Method

The point cloud data measured by the 3D laser scanner was analyzed based on our previous study⁶⁾. As an example, the analysis process using the point cloud data of a block of the 64,000 DWT bulk carrier is explained here. First, the measured point cloud data is processed using FARO SCENE to extract the target rectangular plate. In this stage, the coordinate axes depend on the direction in which the 3D laser scanner is placed, so a coordinate transformation should be performed to align each axis of the orthogonal coordinate system with the longitudinal, transverse, and out-plane directions of the plate. This coordinate transformation is performed by principal component analysis. This means that the first principal component axis with the maximum variance is oriented toward the longitudinal direction, the second principal component axis with the next largest variance is oriented toward the transverse direction, and the third principal component is oriented toward the out-plane direction. A result of the coordinate transformation is shown in Fig. 2. Next, the component analysis of the initial deflection is performed by fitting the deflection modes w_1 to w_5 shown in Fig. 3. w_1 represents the slope of the plane, w_2 represents the twisting mode, w_3 and w_4 represent the overall deflection modes in the longitudinal and transverse directions, respectively, and w_5 represents a local deflection mode indicating the hungry-horse shape, which is the subject of interest in this study. The following equations express these deflection modes:

$$w_1 = c_0 + c_1x + c_2y \quad (1)$$

$$w_2 = c_3xy \quad (2)$$

$$w_3 = \sum_{j=1}^{m_s} \left(\frac{x}{a} B_j + \frac{a-x}{a} C_j \right) \sin \frac{j\pi y}{b} \quad (3)$$

$$w_4 = \sum_{i=1}^{n_s} \left(\frac{y}{b} D_i + \frac{b-y}{b} E_i \right) \sin \frac{i\pi x}{a} \quad (4)$$

$$w_5 = \sum_{i=1}^{m_p} \sum_{j=1}^{n_p} A_{ij} \sin \frac{i\pi x}{a} \sin \frac{j\pi y}{b} \quad (5)$$

where a is the length of the rectangular plate, and b is the width. m_s , n_s , m_p , and n_p are the number of terms considered for each deflection mode. In this study, $m_s = 1$, $n_s = 1$, $m_p = 11$, and $n_p = 3$ are assumed. c_0 , c_1 , c_2 , c_3 , B_j , C_j , D_i , E_i , and A_{ij} are the regression coefficients of each component, and A_{ij} represents the amplitude of the deflection component with i half waves in the longitudinal direction and j half waves in the transverse direction.

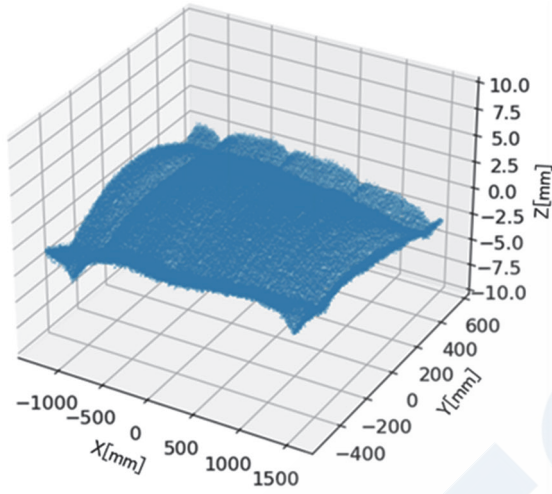


Fig. 2 Point cloud data after coordinate transformation

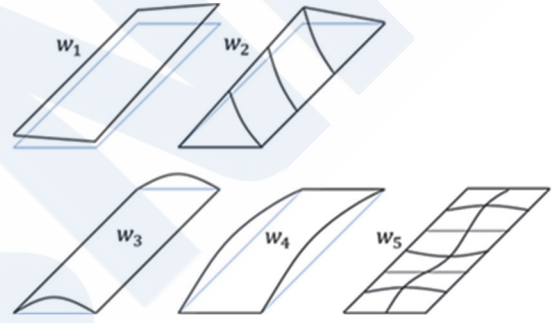


Fig. 3 Superposition of deflection modes

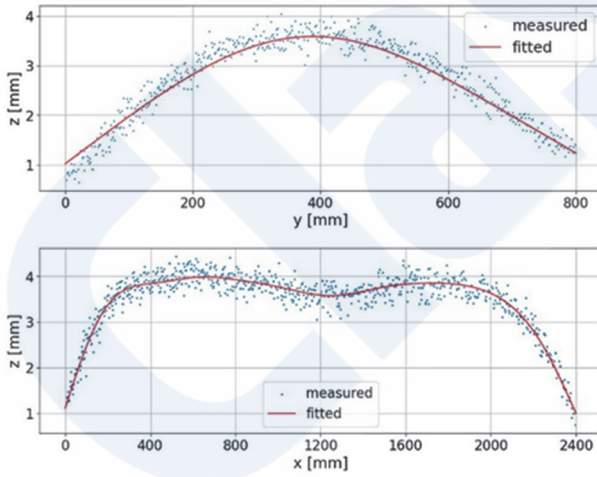


Fig. 4 Measured point cloud and fitted curves

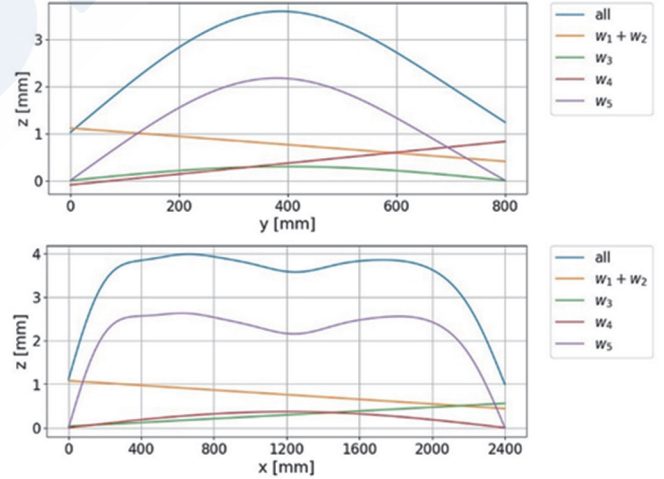


Fig. 5 Mode decomposition of initial deflection

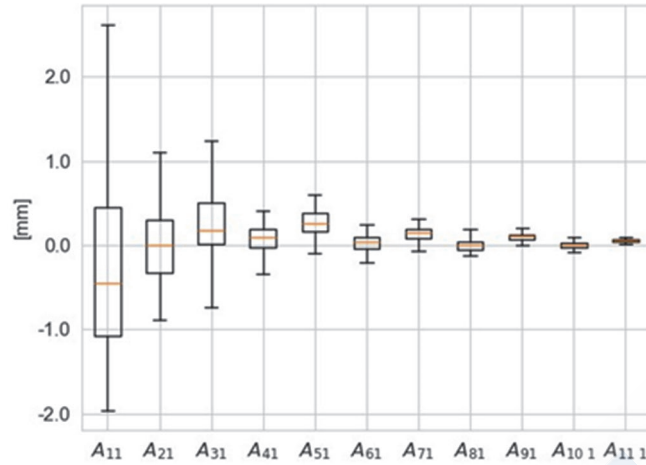


Fig. 6 Initial deflection components

Fig. 4 shows the measured point cloud and the initial deflection curve fitted to the point cloud. Fitting to the point cloud is performed using the least squares method. The x direction is the longitudinal direction of the rectangular plate, the y direction is the transverse direction, and the z direction is the direction in which the stiffeners stand. The fitted curves show the deflection curves along the centerlines of the plate, and the fitted curve generally passes through the center of the point cloud. Fig. 5 shows the result of the component decomposition of the initial deflection. For the target rectangular plate, it is clear that the local deflection mode w_5 is dominant. This series of analyses, from the coordinate transformation to decomposition, is performed for the 62 plates.

3.2 Analysis Results for Single Rectangular Plates

Fig. 6 shows the box plot of A_{i1} ($i = 1$ to 11). It can be seen that the mean values and variances of the odd half-wave components such as A_{11}, A_{31}, A_{51} are larger and more dominant than those of the even half-wave components. However, compared to past measurement results²⁾, a certain number of plates have negative A_{11} . This is because the overall deflection w_4 is predominant in these plates, which results in the negative direction of the local deflection w_5 , as shown in Fig. 7. In other plates, A_{31} and A_{51} are predominant because they have deflection peaks near both ends, leading to the negative A_{11} , as shown in Fig. 8. Further investigation is required to clarify the reason why these initial deflections were induced in the fabrication process.

Fig. 9 shows the relationship between the maximum deflection of the rectangular plate and $\beta^2 t$. β is the slenderness ratio parameter of the plate, expressed as $b/t\sqrt{\sigma_Y/E}$, where b is the width of the plate, t is the thickness of the plate, σ_Y is yield stress, and E is Young's modulus. In addition to the measurement results obtained in this study, past measurement results^{2), 4)} are also shown. The closed dots in the figure represent the results of this study. The straight lines in the figure represent the levels for the maximum initial deflection derived by Smith et al.¹⁰⁾ based on measurements of the initial deflections of actual ships. $0.025\beta^2 t$, $0.1\beta^2 t$, and $0.3\beta^2 t$ were derived as Slight, Average, and Severe deflection, respectively. The maximum values of the initial deflections measured in this study are generally scattered around Slight, and the past measurement results show the same trend.

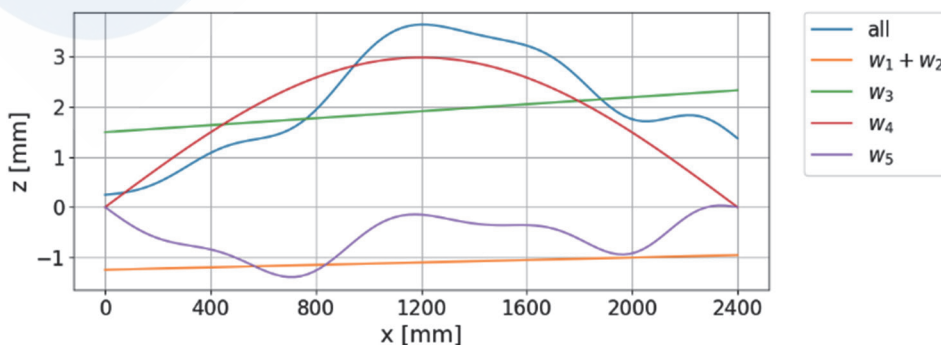


Fig. 7 Initial deflection with predominant overall deflection

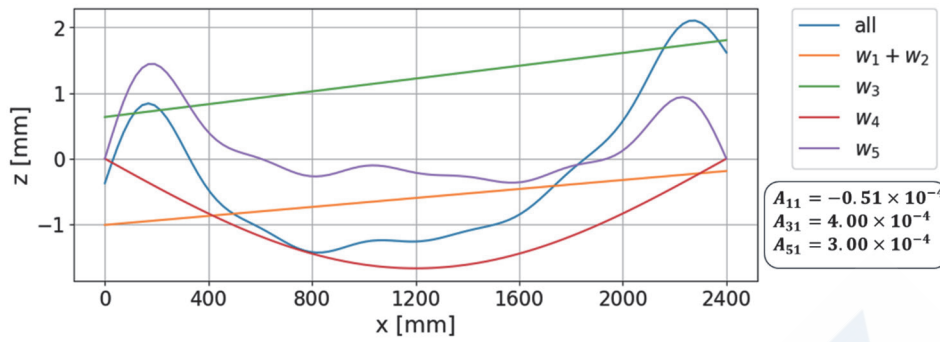


Fig. 8 Initial deflection with two peaks near both ends

3.3 Analysis Results for Adjacent Rectangular Plates

The correlation of the initial deflection between two adjacent rectangular plates is investigated. In addition to the data from the measurements in this study, the data from a 46,000 DWT bulk carrier with the positional relationship of the measured rectangular plates is analyzed.

The two adjacent rectangular plates are referred to as plate P and plate Q. Fig. 10 shows the relationship of A_{11} between plate P and plate Q. The horizontal axis A_{11}^P is one half-wave deflection of plate P, while the vertical axis A_{11}^Q is one half-wave deflection of plate Q. The data are generally distributed along the diagonal line, indicating a positive correlation in A_{11} . The correlation coefficient is 0.62.

Fig. 11 shows the histogram of ΔA_{11} , that is, the difference between A_{11} of the two adjacent plates P and Q. The solid line in the figure represents a fitting normal distribution whose mean is set to zero. The estimated value of the standard deviation is 1.24. It is noted that the KS test is performed and the p-value is above the significance level of 0.05, indicating that the normal distribution hypothesis for A_{11} is not rejected.

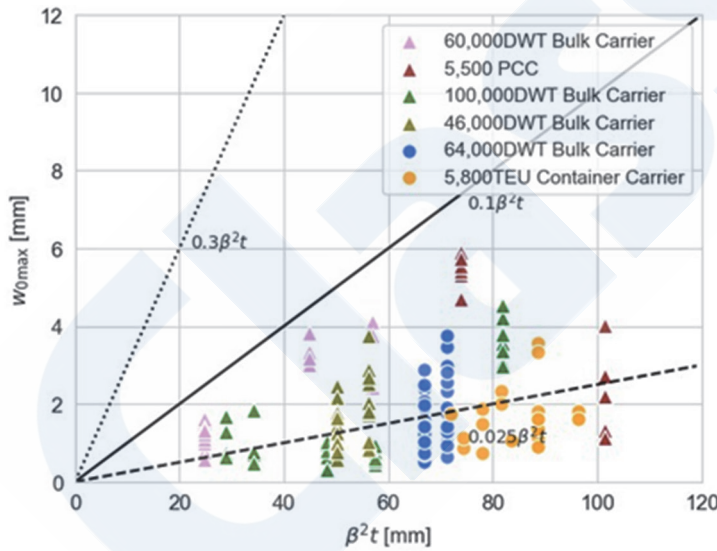


Fig. 9 Maximum values of initial deflection

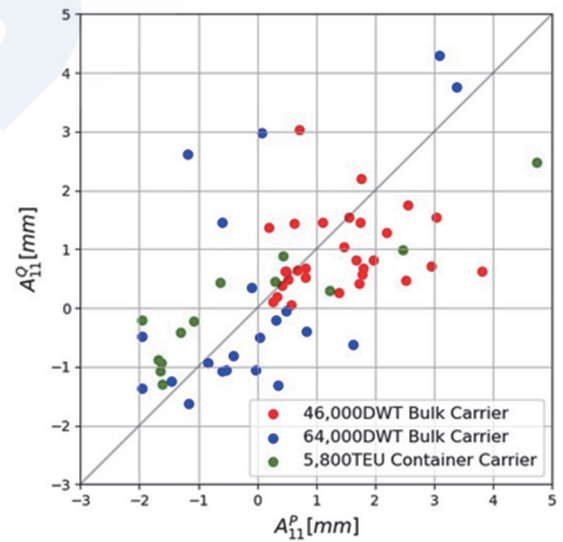


Fig. 10 Comparison of A_{11} of adjacent plates

Next, the maximum deflections of the two adjacent rectangular plates are taken as w_{\max}^P and w_{\max}^Q , and $\alpha = w_{\max}^Q/w_{\max}^P$ ($w_{\max}^P > w_{\max}^Q$), the ratio of the maximum initial deflections, is calculated. Fig. 12 shows the histogram of the initial deflection ratio α . The distribution of α roughly follows a uniform distribution. The average value of α obtained from both the current measurement and the previous measurement of the 46,000 DWT bulk carrier is almost the same, and its value is approximately 0.64.

It is common to assume the initial deflection shape in ultimate strength analyses of stiffened panel structures, and the ultimate strength of a continuous panel is influenced by the antisymmetric component across the stiffener. These results suggest that the maximum initial deflection of plate P is estimated from Fig. 7 and an initial deflection 0.64 times larger than the maximum

deflection of plate P is applied to the adjacent plate Q. This enables an ultimate strength analysis considering the correlation of the initial deflection between the two adjacent rectangular plates.

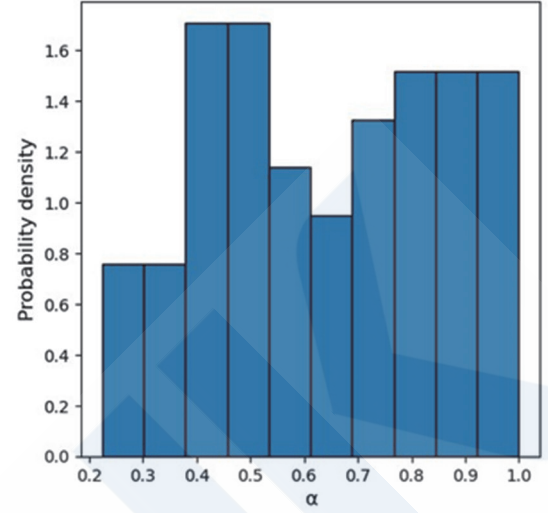
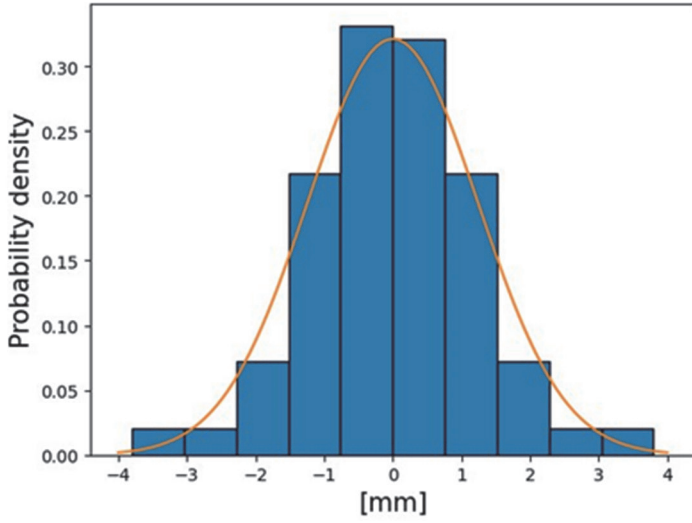


Fig. 11 Histogram of ΔA_{11} and a fitted normal distribution Fig. 12 Histogram of the initial deflection ratio α

4. A STATISTICAL MODEL OF INITIAL DEFLECTION SHAPES CONSIDERING THE CORRELATION OF ADJACENT PANELS

4.1 A Statistical Model for a Single Rectangular Plate

One of the authors proposed a statistical model for predicting the initial deflection shape of a single rectangular plate⁷⁻⁹⁾. In that model, the probability density function of the initial deflection amplitude \mathbf{A} is represented as

$$p(\mathbf{A}) = \frac{1}{\sqrt{(2\pi)^{11}|\boldsymbol{\Sigma}|}} \exp\left\{-\frac{1}{2}(\mathbf{A} - \boldsymbol{\mu})^T \boldsymbol{\Sigma}^{-1}(\mathbf{A} - \boldsymbol{\mu})\right\} \quad (6)$$

$$\boldsymbol{\mu} = \mathbf{c}_0 + \mathbf{c}_1 \left(\frac{b}{t^2}\right) + \mathbf{c}_2 \left(\frac{b}{t^2}\right)^2 \quad (7)$$

The amplitude \mathbf{A} is a vector with the initial deflection amplitudes A_{i1} ($i = 1$ to 11). This model assumes that the initial deflection amplitudes follow a multivariate normal distribution, where the mean $\boldsymbol{\mu}$ is expressed as a quadratic function of the explanatory variable b/t^2 . $\boldsymbol{\Sigma}$ is an 11×11 covariance matrix, b is the plate width, t is the plate thickness, and \mathbf{c}_0 , \mathbf{c}_1 , and \mathbf{c}_2 are vectors of regression coefficients, each with 11 components. The explanatory variable b/t^2 is derived from an existing study on the angular deformation of bead-welded plates¹¹⁾. This statistical model uses Bayesian statistics to estimate the posterior distributions of the parameters \mathbf{c}_0 , \mathbf{c}_1 , \mathbf{c}_2 , and $\boldsymbol{\Sigma}$. In this study, the expected values of the posterior distributions (EAP) of \mathbf{c}_0 , \mathbf{c}_1 , \mathbf{c}_2 , and $\boldsymbol{\Sigma}$ are used as representative values, and the probability density function of the initial deflection of a single rectangular plate is calculated by equations (6) and (7).

4.2 Consideration of Correlation of Adjacent Panels

The statistical model of a single rectangular plate described above in 4.1. is extended to consider the correlation between adjacent plates. The initial deflection components of two adjacent rectangular plates, P and Q, are represented as $\mathbf{A}^P = (A_{11}^P, A_{21}^P, \dots, A_{11}^P)$ and $\mathbf{A}^Q = (A_{11}^Q, A_{21}^Q, \dots, A_{11}^Q)$. The joint probability density distribution of \mathbf{A}^P and \mathbf{A}^Q is proposed as

$$p(\mathbf{A}^P, \mathbf{A}^Q) = p(A_{11}^Q | A_{11}^Q) p(A_{11}^Q | A_{11}^P) p(\mathbf{A}^P) \quad (8)$$

$p(\mathbf{A}^P)$ is the probability density function of the initial deflection components of rectangular plate P given by equation (6), and $p(A_{11}^Q | A_{11}^P)$ represents the conditional probability density function of the one half-wave component of plate Q given the

one half-wave component of plate P. From the results in Fig. 9, assuming that the difference between the one half-wave components $A_{11}^P - A_{11}^Q$ follows a normal distribution with a mean of zero and a standard deviation of σ_d , it can be expressed as

$$p(A_{11}^Q | A_{11}^P) = \frac{1}{\sqrt{2\pi}\sigma_d} \exp\left\{-\frac{(A_{11}^Q - A_{11}^P)^2}{2\sigma_d^2}\right\} \quad (9)$$

Finally, $p(A_o^Q | A_{11}^Q)$ represents the conditional probability density function of the other components $A_o^Q = (A_{21}^Q - A_{11}^Q)$ given A_{11}^Q . Assuming A^Q follows the multivariate normal distribution of equation (6), the conditional distribution is also derived as a multivariate normal distribution:

$$p(A_o^Q | A_{11}^Q) = \frac{1}{\sqrt{(2\pi)^{10} |\Sigma_{o|1}|}} \exp\left\{-\frac{(A_o^Q - \mu_{o|1})^T \Sigma_{o|1}^{-1} (A_o^Q - \mu_{o|1})}{2}\right\} \quad (10)$$

where, $\mu_{o|1}, \Sigma_{o|1}$ are calculated as

$$\begin{aligned} \mu_{o|1} &= \mu_o + \frac{A_{11}^Q - \mu_1}{\sigma_1^2} \sigma_{o1} \\ \Sigma_{o|1} &= \Sigma_{oo} - \frac{\sigma_{o1} \sigma_{o1}^T}{\sigma_1^2} \end{aligned} \quad (11)$$

μ_o is a vector with the 2nd to 11th components of μ , σ_1^2 is an entry in the first row and the first column of Σ , Σ_{oo} is a 10×10 matrix extracted from the 2nd to 11th rows and columns of Σ , and σ_{o1} is a vector extracted from the 2nd to 11th rows of the first column of Σ . Therefore, they are expressed as

$$\begin{aligned} \mu &= \begin{pmatrix} \mu_1 \\ \mu_o \end{pmatrix} \\ \Sigma &= \begin{bmatrix} \sigma_1^2 & \sigma_{1o} \\ \sigma_{o1} & \Sigma_{oo} \end{bmatrix} \end{aligned} \quad (12)$$

Fig. 13 shows the initial deflection shapes of two adjacent plates sampled from the proposed statistical model. Three samples are shown, with the solid line representing rectangular plate P and the dashed line representing rectangular plate Q. By combining the proposed model with the finite element method, it is possible to conduct a Monte Carlo analysis of the ultimate strength of continuous panels with initial deflection.

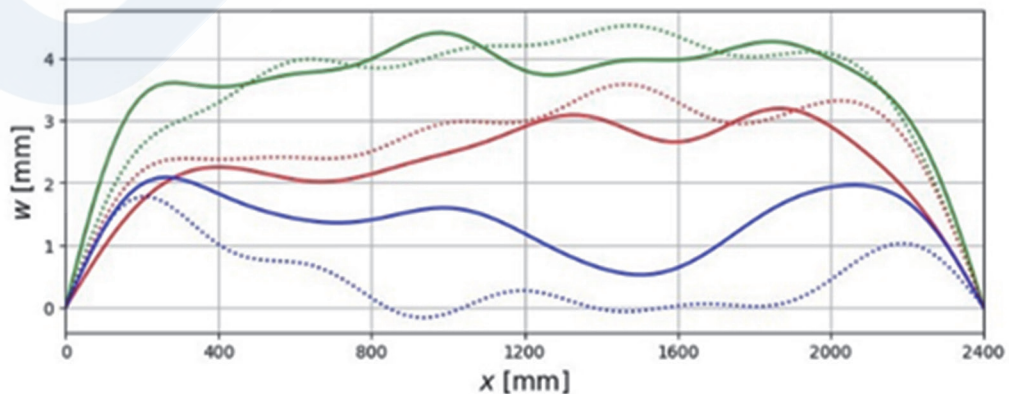


Fig. 13 Sampled initial deflections of adjacent plates

5. CONCLUSION

In this study, the initial deflection shapes of actual ships are measured using a 3D laser scanner, and its applicability is examined. The obtained measurement data are used to analyze the initial deflection components of rectangular plates and to investigate the correlation of the initial deflection components between adjacent plates that affect the buckling and ultimate strength of continuous stiffened panels. A statistical model of the initial deflection of two adjacent plates is developed by extending the existing model of a single rectangular plate. The conclusions are as follows:

- 1) If the positional relationship between the 3D laser scanner and the measurement target is appropriate, the 3D laser scanner can measure the initial deflection of multiple rectangular plates.
- 2) There is a positive correlation in the initial deflection amplitudes with the one-half wave between two adjacent rectangular plates. The average value of the ratio of the maximum initial deflection is approximately 0.64.
- 3) The proposed statistical model can sample initial deflection shapes considering the correlation between adjacent panels.

The initial deflection characteristics measured by the 3D laser scanner are in qualitative agreement with existing measured data, except that a certain number of plates have a negative one half-wave component. Further investigation is needed in this regard.

ACKNOWLEDGMENT

We would like to express our gratitude to Imabari Shipbuilding Co., Ltd. and Nihon Shipyard Co., Ltd for their cooperation in the measurement of the initial deflections.

REFERENCES

- 1) Y. Ueda, T. Yao, The influence of complex initial deflection modes on the behavior and ultimate strength of rectangular plates in compression, *J. of Constructional Steel Research*, **5**, (1985), 265-302.
- 2) T. Yao, M. Fujikubo, Buckling and ultimate strength of ship and ship-like floating structures. *Elsevier*, (2016).
- 3) M. Kmiecik, Jastrze, T. bski, J. Kuzniar: Statistics of ship plating distortions, *Marine Structures*, **8**, (1995), 119–132.
- 4) S. Hirakawa, K. Hayashida, Measurement of initial deflection in stiffened panels and simulation of their buckling/plastic collapse behavior, *Graduation Thesis from the Faculty of Engineering, Hiroshima University*, (1998).
- 5) A. Sano, M. Fujikubo, Buckling Strength of a Non-Spherical Tank in the Partially Filled Condition -part 1: Estimation of the reduction factor due to initial shape imperfection-, *Conference Proceedings, Japan Society of Naval Architects and Ocean Engineers*, **32**, (2020), 117-128.
- 6) A. Tatsumi, Y. Komoriyama, Y. Tanaka, M. Fujikubo, Measurement of Initial Deflection of a Box-Girder Test Model Using 3D Laser Scanner and Its Component Analysis, *Journal of the Japan Society of Naval Architects and Ocean Engineers*, **32**, (2021), 337-342.
- 7) Y. Kageyama, A. Tatsumi, Bayesian Statistics of Welding Initial Deflection of Plate Structure and Its Ultimate Strength Assessment, *Conference Proceedings, Japan Society of Naval Architects and Ocean Engineers*, **32**, (2021), 303-308.
- 8) Y. Kageyama, A. Tatsumi, Bayesian Statistics of Welding Initial Deflection of Plate Structure and Its Ultimate Strength Assessment- Part 2: Effect of Correlation between Initial Deflection Components -, *Conference Proceedings, Japan Society of Naval Architects and Ocean Engineers*, **35**, (2022), 503-505.
- 9) A. Tatsumi, Y. Kageyama, Ultimate strength assessment of rectangular plates subjected to in-plane compression using a statistical model of welding initial deflection, *Marine Structures*, **93**, (2024), 103523.
- 10) C.S. Smith, P.C. Davidson, J.C. Chapman, P.J. Dowling, Strength and stiffness of ships plating under in-plane compression and tension, *Royal Institution of Naval Architects Transactions*, **130**, (1988), 277-296.
- 11) K. Satoh, T. Terasaki, Effect of Welding Conditions on Welding Deformations in Welded Structural Materials, *Journal of the Japan Welding Society*, **45**, (1976), 302-308.